$$v = \frac{b}{\mathrm{tg}\,\Delta\gamma}\,. \qquad (2)$$

If H is the total height of the reconstructed volume, then the number of voxels should be

$$N_{vox} = \frac{H}{h} N_{pix} = \frac{H}{b} tg\,\Delta\gamma\, N_{pix}, \qquad (3)$$

where N_{pix} is a number of pixels in projection.

On the other hand, in algebraic reconstruction technique to calculate the X-ray densities of N_{vox} different voxels, we need at least the equivalent number of equations. When the total angular scanning range is 2γ , the corresponding number of equations is

$$N_{eq} = N_{pix} \frac{2\gamma}{\Delta\gamma} = N_{pix} N_{proj}\,, \qquad (4)$$

where N_{proj} is the total number of projections. From equations **Ошибка! Источник ссылки не найден.**, **Ошибка! Источник ссылки не найден.** and **Ошибка! Источник ссылки не найден.**, we obtain

$$N_{proj} \geq \frac{H}{v} \qquad (5)$$

For instance, if we take angular scanning range $2\gamma = 90^o$, $b = 0.25\,mm$ which corresponds $2\ lp/mm$, and $\Delta\gamma = 1^o$, then $h \approx 14\,mm$ and for $H = 200\,mm$ minimum number of projections, needed for reconstruction, is about 14. Making more projections decreases the relative noise and increases patient dose.

Conclusions. The relationship between the angular scan range and the tomosynthesis slice thickness obtained. Slice thickness appears to be proportional to the in-plane object dimension. The number of projections necessary for the reconstruction of the given number of voxels was calculated. Number of projections is inverse proportional to the projection pixel size.

REFERENCE:

1. Image Artifact in Digital Breast Tomosynthesis and Its Dependence on System and Reconstruction Parameters / *Yue-Houng Hu, Wei Zhao, Thomas Mertelmeier and Jasmina Ludwig* // Digital Mammography. Proc. 9th International Workshop, IWDM 2008 Tucson, AZ, USA, July 20–23, 2008, pp 628–634.

2. *Yue-Houng Hu.* Image artifacts in digital breast tomosynthesis: Investigation of the effects of system geometry and reconstruction parameters using a linear system / *Yue-Houng Hu, Bo Zhao, Wei Zhao* // Medical Physics – 2008 – V. 35(12): 5242–5252.

Submitted on 07.11.14

Мірошниченко С., д-р техн. наук, НВО Телеоптик,
Мотолига О., асп., каф. молекулярної фізики, фізичний факультет,
Київський національний університет імені Тараса Шевченка,
Невгасимий А., канд. техн. наук, НВО Телеоптик, Сенчуров С., канд. фіз.-мат. наук,
каф. молекулярної фізики, фізичний факультет,
Київський національний університет імені Тараса Шевченка

ТЕОРЕТИЧНА ОЦІНКА ТОВЩИНИ РЕКОНСТРУЙОВАНОГО ЗРІЗУ ПРИ ЦИФРОВОМУ ТОМОСИНТЕЗІ

Представлено теоретичну оцінку залежності товщини реконструйованого зрізу при цифровому томосинтезі від куту розвороту. Показано залежність товщини зрізу від розміру об`єкту в площині зрізу.

Ключові слова: *Цифровий рентгенівський томосинтез, товщина зрізу, медичні зображення.*

Мирошниченко С., д-р техн. наук, НПО Телеоптик,
Мотолыга А., асп., каф. молекуляной физики, физический факультет,
Киевский национальный университет имени Тараса Шевченко,
Невгасимый А., канд. техн. наук, НПО Телеоптик, Сенчуров С., канд. физ.-мат. наук,
каф. молекуляной физики, физический факультет,
Киевский национальный университет имени Тараса Шевченко

ТЕОРЕТИЧЕСКАЯ ОЦЕНКА ТОЛЩИНЫ РЕКОНСТРУИРОВАННОГО СРЕЗА ПРИ ЦИФРОВОМ ТОМОСИНТЕЗЕ

Представлено теоретическую оценку толщины реконструированного среза при цифровом томосинтезе в зависимости от угла разворота. Показано зависимость толщины среза от размера объекта в плоскосте среза.

Ключевые слова: *Цифровой рентгеновский томосинтез, толщина среза, медицинские изображения.*

УДК 620.18:546.28

N. Nakhodkin, Dr. Sc., Prof., acad. of NAS of Ukraine,
N. Kulish, Dr. Sc., Prof., Member of NAS of Ukraine, Taras Shevchenko National University of Kyiv
P. Lytvyn, Ph.D., Lashkaryov Institute of Semiconductor Physics, National Academy of Sciences of Ukraine
T. Rodionova, Ph.D., A. Sutyagina., stud., Taras Shevchenko National University of Kyiv

SPECIAL JOINTS OF GRAIN BOUNDARIES IN NANOSILICON FILMS WITH EQUIAXED AND FIBROUS STRUCTURES

Atomic force microscope was used for investigation of grain boundaries joints in undoped nanoysilicon films. It was shown that in films with equiaxed and fibrous structure joints differ in the number and mutual arrangement of special boundaries $\Sigma = 3^n$ and of the general type boundaries.

Key Words: *nanosilicon films; structure; joints of grain boundaries*

Introduction. Nanosilicon films are one of the leading electronic materials for large-area application as solar cells or switching electronics used for flat-panel displays. As is known [3, 8], the characteristics of the electronic devices that use nanosilicon films are directly connected with the structural properties of the films, in particular, their grain boundary and grain boundary joints. Grain boundary joints in a polycrystalline microstructure correspond to the one-dimensional regions of space where three or more grain boundaries meet. In total volume of nanocrystalline material part of the grain boundaries and joints of grain boundaries is ≥ 50%. It is evident that the joints influence the film structure formation and properties of the films. This effect is different for various joints and is structure-dependent.

Of particular interest is the investigation of special grain boundary joints that result from interaction of special grain boundaries. These joints possess a low energy, weak trend to impurity adsorption, low diffusive penetration and so on. As compared to joints of general type, the special joints are more stable, because mobility of special grain boundaries is low [2].

It is well known [5] that in thick polysilicon films (≥ 500 nm), relative amount of special joints is defined by the film structure type (equiaxed, dendritic, fibrous). As for undoped nanosilicon films, in previous studies it has been shown [4] that there are two structural modification of nanosilicon films, depending on their thickness, namely, equiaxed (at thickness < 70 nm) and fibrous (at thickness ≥ 70 nm). It is reasonably to suggest that grain boundary structures of these films are different.

In this work grain boundaries joints in undoped equiaxed and fibrous nanosilicon films were investigated by atomic force microscope (AFM)

Experimental procedure. Nanosilicon films were prepared by low-pressure chemical vapour deposition from a silane/argon mixture. Films were deposited on thermally oxidized (100) single-crystal silicon wafers. The deposition temperature was equal to 630^0C. The film thickness was ranged from 3 to 100 nm.

AFM has been used to obtain a set of statistical data in studies of grain boundary joints. The film surface images were obtained using a scanning atomic force microscope NanoScope IIIa in the periodic contact mode.

Joints attributed to one or another type, depending on the joint configuration and, more importantly, depending on the angles between grain boundaries that form the joint. The values of angles were compared with the values of the angles between the corresponding crystallographic planes [9] and the values of the angles between the twins of different orders [2] in the face-centered cubic lattice.

Results and Discussion. AFM studies show that several types of triple and multiple joints are observed in nanosilicon films. These joints differ by grain boundary orientation.

AFM-images and corresponding schematic drawing in Table 1 show several types of triple grain boundary joints in nanosilicon films. The following types of triple joints were observed:

1. 3a joint is a contact of three grain boundaries of general type (GBGT). Dihedral angles between boundaries can be arbitrary, and in equilibrium state close to 120^0.

2. 3b joint is a contact of two GBGT grain boundaries and twin boundary Σ=3 (Σ is the inverse density of coincidence sites in the coincidence site lattice (CSL) [5]). Dihedral angles between GBGT boundaries close to 180^0.

3. 3c joint is a contact of three coherent twin boundaries $\Sigma=3^n$. This joint is discussed in detail in [6].

***Table* 1**

Types of triple joints in nanosilicon films

Joints type	3a	3b	3c
AFM-images	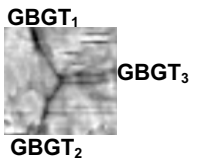	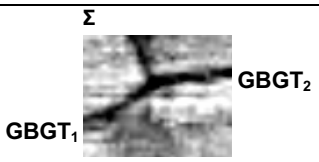	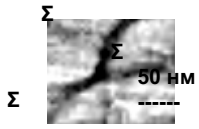
Schematic drawing	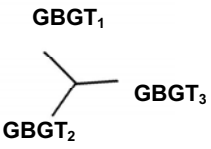	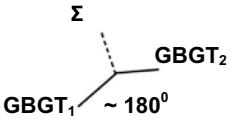	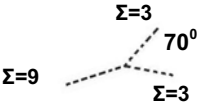
– grain boundaries of the general type (GBGT); – special grain boundaries (Σ)			

***Table* 2**

Types of multiple joints in nanosilicon films

Joint type	4a	4b	4c	5d
AFM images	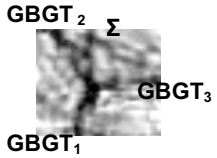	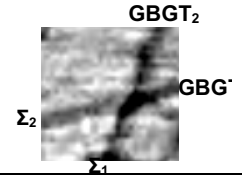		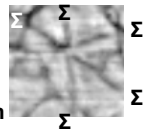
Schematic drawing	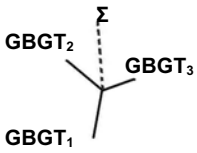	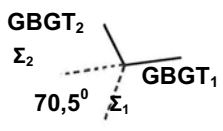	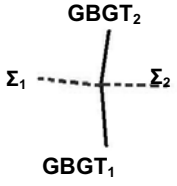	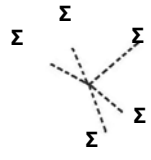
– grain boundaries of the general type (GBGT); – special grain boundaries (Σ)				

Joints, in which four or more grain boundaries meet (multiple joints), were considered in [2,5] for metals and thick (thickness ≥ 500 nm) polysilicon films, respectively. Table 2 represents AFM-images and corresponding schematic drawing of multiple joint types for nanosilicon films. The following types of multiple joints were observed:

1. 4a joint is a contact of three GBGT boundaries and twin boundary Σ = 3. In this case the line of joint lies along the close-packed directions [110], [211], [321].

2. 4b joint is a contact of two GBGT grain boundaries and two coherent twin boundaries Σ = 3. As bypassing the joint following alternation takes place: $GBGT_1 \rightarrow \Sigma = 3_1 \rightarrow \Sigma = 3_2 \rightarrow GBGT_2$. Joint line is always lies along the [110] direction, which is the intersection of the {111} planes of coherent twin boundaries $\Sigma = 3_1$ and $\Sigma = 3_2$. Dihedral angle between the boundaries Σ = 3 is 70.5^0, or 109.5^0. The angle between the $GBGT_1$ and $GBGT_2$ boundaries is generally much less than 180^0.

3. 4c joint is a contact of two GBGT grain boundaries and two coherent twin boundaries Σ = 3. However, unlike the junction 4b, alternation of boundaries another: $GBGT_1 \rightarrow \Sigma = 3 \rightarrow GBGT_2 \rightarrow \Sigma = 3$. Dihedral angle between the Σ = 3 boundaries can be arbitrary. Joint line strictly coincides with the [211], [321], [431], but [110] direction never found.

4. 5d joint. The interaction between the boundaries $\Sigma = 3^n$ creates joints of five boundaries 5d, among which the most widespread is: $\Sigma = 3 \rightarrow \Sigma = 3 \rightarrow \Sigma = 3 \rightarrow \Sigma = 3 \rightarrow \Sigma = 81$. 5d joints line is always lies along the direction [110], which is common to all boundaries in joint [5].

Analysis of AFM images shown that the relative number of various types of grain boundary joints changes under transformation from equiaxed film structure to fibrous. Fig. 1 shows the changes in the relative number of triple and multiple joints with increasing the film thickness from 10 nm to 100 nm. As is seen from the Fig. 1, for all films thickness that was tested, the number of triple junctions dominates. Analysis of statistical data shows that at the early stages of film growth (d = 100 nm), the relative number of multiple joints of all types is only 15% (Fig. 1).

As shown above (Table. 1 and Table 2), triple and multiple joints differ from one another by the number of boundaries of general type and special ($\sum = 3^n$) boundaries. Fig. 2 shows the thickness dependence of relative number of different types of triple and multiple joints. With film thickness increasing number of special boundaries increases and the boundaries of general type is reduced. Thus, the decrease of free surface energy under film growth is not only by reducing the surface area of the grain boundaries, but also by the quality of the boundaries. Primarily disappear boundaries of general type, which have a high specific surface energy, and special boundary are the longer, the lower their energy [1] We can assume that this increasing in the relative number of special boundary $\Sigma = 3^n$ causes the increase in the number of joints of special type 3b and 3c, as well as multiple joints of all types. It can be assumed that the increasing in the relative number of chance meeting of special boundaries between themselves and with the boundaries of the general type leads to an increasing in the relative number of special multiple joints. For films with a thickness of 50 nm it is 35 %.

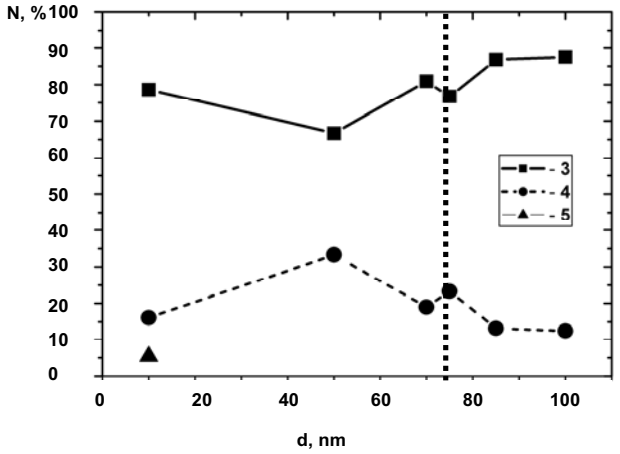

Fig. 1. The relative number of triple and multiple grain boundaries joints in nanosilicon films, depending on the film thickness (dashed line separates the areas of film thickness of equiaxed (d < 70 nm) and fibrous (d ≥ 70 nm) structures)

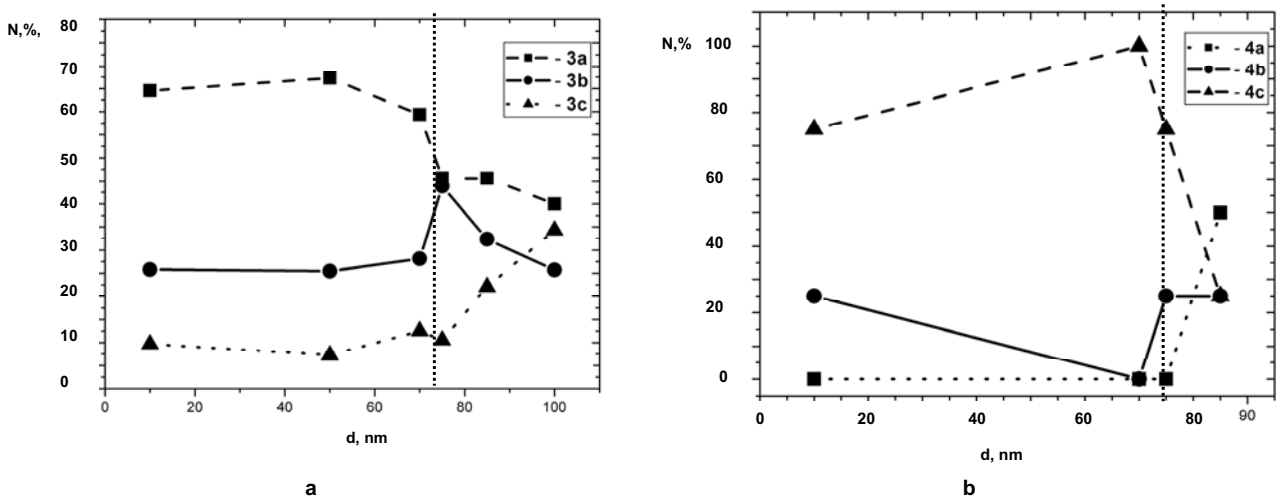

Fig. 2. The relative number of different types of triple (a) and multiple (b) grain boundaries joints in nanosilicon films, depending on the film thickness (dashed line separates the areas of film thickness of equiaxed (d < 70 nm) and fibrous (d ≥ 70 nm) structures)

Attention is drawn to the fact that in equiaxed nanosilicon films (film thickness < 70 nm) joint lines lie along different directions, in particular, [211], [321], [431], [110]. This correlates with the absence of texture in these films. At the same time, in fibrous films (thickness ≥ 70 nm) joint lines always coincide with the direction [110], which correlates with the presence of preferred orientation [110] in these films [7].

Conclusions

1. Triple and multiple joints of grain boundaries are observed in nanosilicon films. Crystallographic classification of multiple joints carried out.

2. As triple and multiple grain boundaries joints are divided in joints of general type and special joints.

3. There are several types of special grain boundaries joints, which differ in the number and mutual arrangement of special boundaries $\Sigma = 3^n$.

4. In films with equiaxed structure (thickness < 70 nm) joint lines lie along different directions, in particular, [211] [321] [431] and [110] that corresponds to a disordered film structure.

5. In films with fibrous structure (thickness ≥ 70 nm) joint lines coincide that correlates with the presence of texture [110] in these films.

REFERENCE:

1. *Dillon S. J.* Mechanism for the development of anisotropic grain boundary character distributions during normal grain growth / S. J. Dillon, G. S. Rohrer // Acta Materialia, 2009. – Vol. 57, – P. 1–7.

2. *Kopetsky Ch. V.* Grain boundaries in pure materials / Ch. V. Kopetsky, A. N. Orlov, L. K. Fionova – Moskow: Nauka, 1987. – 158 p. [in Russian].

3. *Mukhopadhyay S.* Nanocrystalline silicon: A material for thin film solar cells with better stability / S. Mukhopadhyay, A. Chowdhury, S. Ray // Thin Solid Films, 2008. – Vol. 516, Issue 20. – P. 6824–6828.

4. *Nakhodkin N. G.* Effect of thickness on structural characteristics of nanosilicon films / N. G. Nakhodkin, N. P. Kulish, T. V.Rodionova, A. S. Sutyagina // Bulletin of Taras Shevchenko National University of Kyiv Series Physics & Mathematics, 2012. – V. 1. – P. 285–288.

5. *Nakhodkin N. G.* Troinye i mnozestvennye spetsialnie styki zeren v polikremnievych plenkach s raznym tipom struktury / N. G. Nakhodkin, N. P. Kulish, P. M. Lytvyn, T. V.Rodionova // in Coll. of Sci. works on Nanosystems, Nanomaterials, Nanotechnologies, Kiev,2004. – V. 2, № 3. – P. 793–801.

6. *Costantini S. Cleri F.* Triple junctions and elastic stability of polycrystalline silicon / S. Costantini, P. Alippi, L. Colombo / Phys. Rev. B, 2001. – Vol. 63, Issue 4. – P. 045302-1–045302-4.

7. *Nakhodkin, N. G.* Formation of different types of polysilicon film structures and their grain growth under annealing / N. G. Nakhodkin, T. V. Rodionova // Phys. Status Solidi A., 1991. – Vol. 123, № 2. – P. 431–439.

8. *Rath J. K.* Low temperature polycrystalline silicon: a review on deposition, physical properties and solar cell applications / J. K. Rath // Sol. Energy Mater. Sol. Cells., 2003. – Vol. 76, № 4. – P. 431–487.

9. *Хирш П.* Электронная микроскопия тонких кристаллов / П. Хирш, А. Хови, Р. Николсон, Д. Пэшли, М. Уэлан / Пер. с англ. Под ред. Утевского Л.М. – М.: Мир,. 1968. 574 с.

Submltted on 20.03.14

Находкін М., д-р фіз.-мат. наук, проф., акад. НАНУ, Куліш М., д-р фіз.-мат. наук, проф., чл.-кор. НАНУ,
Київський національний університет імені Тараса Шевченка,
Литвин П., канд. фіз.-мат. наук, Інститут фізики напівпровідників імені В. Є. Лашкарьова НАН України,
Родіонова Т., канд. фіз.-мат. наук, Сутягіна А., студ.,
Київський національний університет імені Тараса Шевченка

СПЕЦІАЛЬНІ СТИКИ ГРАНИЦЬ ЗЕРЕН У НАНОКРЕМНІЄВИХ ПЛІВКАХ З РІВНООСЬОВОЮ ТА ВОЛОКНИСТОЮ СТРУКТУРОЮ

Методами атомної силової мікроскопії досліджено спеціальні стики границь зерен в нанокремнієвих плівках. Показано, що в плівках з рівноосьовою та волокнистою структурою стики відрізняються кількістю та взаємним розташуванням спеціальних границь $\Sigma = 3^n$ та границь загального типу.

Ключові слова: *нанокремнієві плівки; структура; стики границь зерен*

Находкин Н., д-р физ.-мат. наук, проф., акад. НАНУ, Кулиш Н., д-р физ.-мат. наук, проф., чл.-кор. НАНУ,
Киевский национальный университет имени Тараса Шевченко,
Литвин П., канд. физ.-мат. наук, Институт физики полупроводников имени В. Е. Лашкарева НАН Украины,
Родионова Т., канд. физ.-мат. наук, Сутягина А., студ.,
Киевский национальный университет имени Тараса Шевченко

СПЕЦИАЛЬНЫЕ СТЫКИ ГРАНИЦ ЗЕРЕН В НАНОКРЕМНИЕВЫХ ПЛЕНКАХ С РАВНООСНОЙ И ВОЛОКНИСТОЙ СТРУКТУРОЙ

Методами атомной силовой микроскопии исследованы стыки границ зерен в нанокремниевых пленках. Показано, что в пленках с равноосной и волокнистой структурой стыки отличаются количеством и взаимным расположением специальных границ $\Sigma = 3^n$ и границ общего типа.

Ключевые слова: *нанокремниевые пленки; структура; стыки границ зерен*

UDC 53; 547.136.13; 576.535; 577.037

Ye. Oberemok, Ph.D.
Department Quantum Radiophysics,
Faculty of Radio Physics, Electronics and Computer Systems
Taras Shevchenko National University of Kyiv

THE MUELLER MATRIX STRUCTURE OF MEDIA WITH ORTHOGONAL EIGENPOLARIZATIONS

The Mueller matrix structure and relationships between its elements for media with orthogonal eigenpolarizations were studied. Relations has been derived were verified on basic types of anisotropy and mixtures of ones. It was shown that Mueller matrix of medium with orthogonal eigenpolarizations has less than twelve independent elements. In addition the conditions which determine the values of anisotropy parameters for the eigenpolarizations to be orthogonal have been derived and examined for several characteristic mixtures of anisotropies. In particular it was founded that the orthogonality of eigenpolarization is always possible in mixtures of four basic types of anisotropy by properly fitted birefringent part. Finally the symmetry of the Mueller matrix, resulted from eigenpolarizations orthogonality, was established and analyzed for optimal measurement.

Keywords: *Mueller matrix, eigenpolarizations orthogonality, parameters of anisotropy.*

Introduction. It is well known that in optics and electrodynamics the crystalline medium are characterized by the types of eigenpolarizations that this medium possesses. Eigenpolarizations are those polarization states of light that do not change when passing through a medium. The amplitude and the overall phase of the beam of light with an eigenpolarization do, however, change. These changes are described by the corresponding